

VDES R-Mode performance analysis and experimental results

Markus Wirsing  | Armin Dammann  | Ronald Raulefs 

Institute of Communications and Navigation,
German Aerospace Center, Weßling, Germany

Correspondence

Markus Wirsing, Institute of Communications
and Navigation, German Aerospace Center
(DLR), Weßling, Germany.
Email: Markus.Wirsing@dlr.de

Funding information

Interreg; European Union

Summary

Global Navigation Satellite Systems (GNSS) have become an essential part of maritime navigation, in particular to improve situational awareness and vessel traffic management. The dependence on GNSS creates vulnerability for maritime shipping. Driven by this vulnerability, the desire for a backup system for maritime navigation has been emerging. The VHF Data Exchange System (VDES) standard provides communication capabilities for maritime applications. VDES is currently being revised. As part of this revision, VDES will be extended by ranging and navigation functionalities, called R-Mode, as an alternative for maritime navigation. In this paper, we address system design aspects and evaluate the positioning performance of VDES R-Mode. We derive estimation theory bounds on the accuracy of VDES R-Mode distance and velocity. In a case study, we discuss and evaluate the benefit of satellite links to complement VDES R-Mode positioning. Furthermore, we introduce a Kalman filter for position and velocity tracking, which we apply to experimental data. We describe an experiment we conducted at Lake Ammer, southwest of Munich, and evaluate the VDES R-Mode positioning performance for this setup. Our experimental results show that VDES R-Mode is capable of achieving a 95th-percentile horizontal position error of 22 m. Thus, VDES R-Mode is a promising approach for a maritime backup system that can meet the IALA accuracy requirements.

KEYWORDS

alternative PNT, Cramér–Rao bound, experimental validation, Kalman filter, maritime navigation, VDES, VDES R-Mode, Ziv–Zakai bound

1 | INTRODUCTION

Modern maritime traffic relies on Global Navigation Satellite Systems (GNSS) for navigation purposes. Satellite systems provide an accurate position estimate that fulfills the requirements for maritime traffic, but they are not entirely free of failures. Jamming and spoofing attacks on GNSS increasingly occur, and the recent outage of the Galileo navigation system serves as a reminder that the systems themselves can experience outage.¹ For these reasons, it is desirable to have a secondary source to estimate the position while out at sea.

In this paper, we present an approach to utilize the VHF Data Exchange System (VDES), that is currently in the process of being standardized at the International Telecommunications Union (ITU), as an alternative navigation system to GNSS. VDES comprises a terrestrial (VDE terrestrial) and a satellite (VDE satellite) communication component and is expected to provide communication coverage around the world. VDE terrestrial is foreseen to cover coastal areas and ports, which are today covered by AIS base stations (BSs). VDE satellite provides communication access to the open sea and arctic areas.

This is an open access article under the terms of the Creative Commons Attribution License, which permits use, distribution and reproduction in any medium, provided the original work is properly cited.

© 2021 The Authors. *International Journal of Satellite Communications and Networking* published by John Wiley & Sons Ltd.

Extending a communication system, like VDES, by a ranging component (R-Mode), permits a VDES receiver to additionally estimate the distance between the transmitter and the receiver that is located on the ship. If a sufficient number of transmitters are available, the receiver can determine the position by multilateration. In case the number of received signals is not sufficient for an ambiguity free determination of the position, the obtained information can still be utilized to verify the integrity of GNSS. The VDES R-Mode concept is described in reference,² and literature³ explains how it utilizes the VDES communication system.

The concept of R-Mode was first considered in 2008. The considered concept relied on utilizing existing maritime communication infrastructure such as the MF radio beacon and AIS⁴ and is outlined in the report of the IMO subcommittee as part of the IMO e-Navigation strategy.⁵ In 2014, the ACCSEAS project analyzed the theoretical ranging performance of the MF radio beacon system⁶ as well as the AIS.⁷ In literature,⁸ the authors evaluated the positioning performance and heading errors based on a single AIS shore station and with multiple antennas at the Chinese sea. To overcome the limitations of limited bandwidth of the AIS versus VDE terrestrial, the authors in reference⁹ assessed the ranging performance from one to five AIS slots. They compared the performance with different bandwidth allocation for a one slot message of VDE terrestrial. The ranging performance for VDE terrestrial with 100-kHz bandwidth was superior compared with a multislot AIS ranging message. A further concern about the use of AIS is the heavy communication load that the AIS network experiences in busy regions already today. Therefore, additional messages that are regularly transmitted would exacerbate the risk of overloading the AIS network and, therefore, impair the situational awareness.

The paper is structured as follows: Section 2 introduces the development of navigation systems to complement satellite-based ones by utilizing a communication system. Section 3 describes the VDES system, and how VDES R-Mode is expected to utilize it. Section 4 derives the theoretical bounds and provides simulations for the terrestrial VDE communication link on ranging and velocity estimation. Further, the estimated range and velocity are fused in a Kalman filter to track the position of the receiver. Because terrestrial BSs are built up along the coastline, the resulting adverse geometric constellations of BSs limit the positioning performance. Therefore, we assess the potential impact of using the VDES satellite communication link as an additional ranging link. The terrestrial system has been assessed and evaluated by measurements on the Lake Ammer. In Section 5, the measurement setup is introduced and results are provided. In Section 6, the measurement results are discussed to evaluate for the first time the positioning performance of VDES R-Mode.

2 | RADIO NAVIGATION SYSTEMS

In the following, we summarize selected developments in radio navigation that are relevant to understanding the motivation and development of VDES R-Mode as a contingency radio navigation system for the mariner. It is relevant to understand the difference of alternative navigation systems to GNSS. In literature,¹⁰ three levels are identified: first, a redundant system that fulfills the same requirements all the time everywhere in case of a GNSS failure and does not need to change any procedures; second, a backup radio navigation system that replaces the existing radio navigation system in case of a failure and fulfills the relevant requirements; and third, a contingency radio navigation system that fulfills less stringent requirements than the operational radio navigation system and may require to change procedures for safety reasons for a limited duration. Radio navigation either utilizes a communication network or is set up as a dedicated system. Terrestrial navigation systems that cover a large area were superseded by satellite systems, namely, GPS (NAVSTAR global positioning system) in the 1990s. Especially in 2000 after selective availability of GPS was turned off, the performance available to civilian users increased substantially.

GPS and all other satellite navigation systems rely on navigation data that are included in the data stream. In 2004, the navigation data for GPS were successfully provided via mobile radio networks for the first time. This service is called assisted-GPS (A-GPS). In VDES R-Mode, it is currently foreseen that the VDES network provides the navigation data via its terrestrial part. However, VDES R-Mode could utilize satellite VDE in areas where data communication can no longer be reliably provided by the terrestrial network part.

2.1 | LORAN and GPS

During the second world war, the LORAN (long range navigation) system was developed as a terrestrial maritime radio navigation system. LORAN was refined and optimized during the decades afterwards. The ubiquitous availability and success of GPS led to the demise of LORAN in multiple countries around the world. However, the strong interdependence of GPS with all navigation and communication systems on-board led to a reconsideration of a terrestrial navigation system, at least as a contingency radio navigation and timing system.¹¹ The successor enhanced LORAN (eLORAN) gained interest and provides a significantly improved performance, but its future service remains uncertain.

2.2 | The role of mobile radio communication systems

At the end of the 1990s and based on the request of the Federal Communications Commission (FCC) in the United States, navigation capabilities using the cell-ID were added to cellular mobile radio devices on land. The FCC demanded that the cellular network provider must be capable of locating the mobile device in case of an emergency call (911) to improve safety. The improved availability of GPS in the year 2000 and the development of future satellite-based navigation systems moved the focus of the cellular network providers towards exploiting the satellite navigation systems. A major challenge was the high time to first fix (TTFF) for position calculation in a mobile device. Therefore, for 3G networks, A-GPS as an additional service was standardized to assist GPS by providing navigation data about the navigation satellites through the communication data link of the cellular network provider to improve the cold start capabilities significantly^{12,13} from several minutes to seconds. Further research to utilize the radio communication link itself to determine the position took off. In the LTE standard Release 8, the radio communication link provides additional pilots to improve the determination of the position of the mobile device in the network.¹³

2.3 | MF R-Mode

A second maritime contingency navigation system operating in the MF-band is currently under development and called MF R-Mode. MF R-Mode will cover a larger area¹⁴ than VDES R-Mode, but comes with a poorer position performance. Further, a crucial drawback is the additional degradation of the position performance by an order of magnitude during nighttime due to the sky-wave effect. The MF R-Mode system utilizes the carrier phase of the IALA beacon system with two added continuous wave signals. The two carriers are added at an offset of ± 225 Hz to the carrier of the MSK signal used for DGNSS corrections and thus within the allocated channel bandwidth of 500 Hz.

A dedicated carrier is added to the outer band¹⁵ to optimize the ranging performance with the available spectrum. In the future, MF and VDES R-Mode can complement each other as a joint system in terms of coverage and availability, especially along major cargo routes around the globe.¹⁴

3 | VDE AND VDES R-MODE

VDES R-Mode is a navigation application that utilizes mainly the terrestrial VDE component of the VDES communication system. In this section, we introduce the VDE system as a communication system, and the VDES R-Mode navigation application.

3.1 | The VDE system

The VHF Data Exchange System (VDES) was standardized by ITU in 2015 (ITU-R M.2092)¹⁶ and is currently being revised in ITU WP5B. The standard is built on the IALA Guideline G1139³ and has been developed since 2009 at IALA. It comprises three communication systems: the Automatic Identification System (AIS), the Application Specific Message (ASM) system, and the terrestrial and satellite VHF Data Exchange (VDE-T and VDE-S).

AIS is an already existing system that is a part of the VDE System and is standardized separately in ITU-R M.1371.¹⁷ The vessels regularly broadcast information about their position, heading, and velocity. Therefore, it serves as an important tool to increase situational awareness. AIS utilizes two separate 25-kHz channels, applies no forward error correction, and relies on GMSK modulation. Further objectives of AIS are to obtain information about the vessel and its cargo and to provide information that is used in dense areas for traffic monitoring and management by vessel traffic systems.

The ASM system broadcasts messages that are not required to increase the situational awareness. Its purpose is to reduce the load in the AIS network. The VDES standard describes a portfolio of messages that use one to three ASM time slots. ASM applies forward error correction and, therefore, achieves an improved reception quality for terrestrial and satellite reception compared with AIS.

VDE comprises a terrestrial and a satellite communication link. The VDE-T data link is used for general data that is either exchanged between shore and vessel or between vessels. The VDE-S data link provides bidirectional communication between vessels and VDE satellites. The allocated spectrum for VDE-T consists of 100 kHz for the downlink and another frequency band of 100 kHz for the uplink. The allocated spectrum for VDE-S covers up to 150 kHz and fully overlaps with both VDE-T frequency bands. The transmit power of the satellite is 30 dBm EIRP and, therefore, significantly weaker than the VDE-T transmit power level of up to 41 dBm, which still excludes potential antenna gains on the transmitter side. Therefore, a detrimental interference of VDE-S on VDE-T is not expected in the service area of VDE-T. VDE-S provides the crucial communication coverage beyond VDE-T, for example, on the open sea.

The VDE-T link utilizes modulation schemes, such as $\pi/4$ -QPSK and 16-QAM, and applies forward error correction. Figure 1 shows the $\pi/4$ -QPSK modulation scheme that is used also for VDES R-Mode. Data are transmitted within time slots of 26.67 ms duration. The transmission scheme of multiple BSs is coordinated by the network provider in a defined service area to avoid interfering messages at the receiver.

The slots are organized by the network, and resources are assigned in the bulletin board every 60 s. For VDE-T, the data package consists of a ramp up sequence, followed by a synchronization sequence, configuration data, the message data, and finally closed by the ramp down sequence.

3.2 | The VDES R-Mode application

The VDES R-Mode application provides a system for Positioning, Navigation and Timing (PNT) for maritime shipping. The operational concept is that, in the event of a disruption to GNSS services on-board a ship, the VDES R-Mode system (possibly together with other terrestrial PNT systems such as MF R-Mode and eLORAN) provides ranging measurements to an on-board navigation system to mitigate the impact of the GNSS service outage on the ship's ability to navigate safely, especially in coastal areas and for harbor approaches.

The VDES R-Mode system will transmit accurately timed ranging signals from a network of land-based and possibly offshore BSs in the VHF band. The VDES R-Mode receiver measures the timing (and other) parameters of the received signals and outputs the signal observables to an external PNT unit, such as the Multi-system Shipborne Radionavigation Receiver (MSR) described in literature.¹⁸ The IALA Guideline G1158² outlines the VDES R-Mode system setup as follows. The PNT unit utilizes these observables to determine the vessel's position, speed over ground, and other navigation parameters. VDES R-Mode should, as far as possible, use preexisting infrastructure, including shore stations, monitoring and control centers, and preexisting AIS/VDES shipborne installations. Monitoring and control data are likely to be carried between the BSs, far-field monitoring stations, and monitoring and control stations via preexisting wide area networks. VDES R-Mode will be synchronized to an external time source traceable to a common time scale in order to facilitate interoperability with other PNT systems. The ranging sequence is predefined and consists of an alternating sequence and a Gold code sequence. The ratio of both sequences is communicated prior

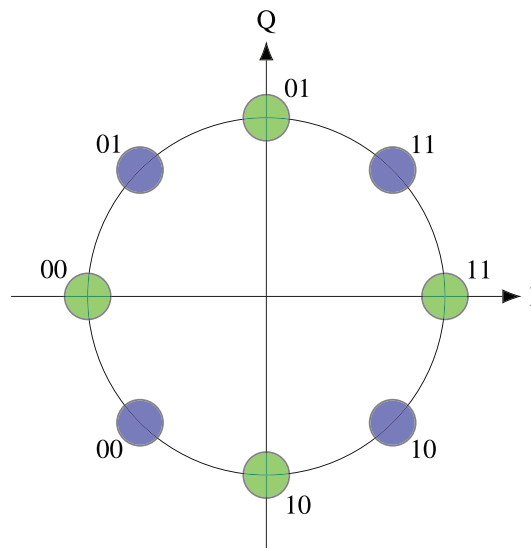


FIGURE 1 $\pi/4$ -QPSK modulation alphabet and mapping to data bits. A phase shift of $\pi/4$ rad is applied at every second time instance

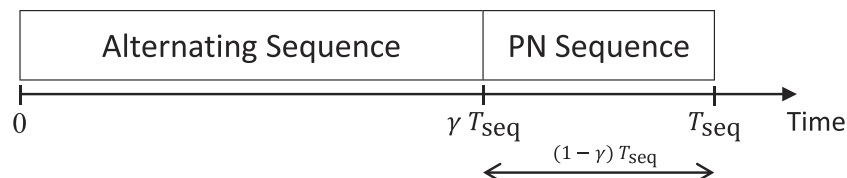


FIGURE 2 The ranging sequence is split into two parts consisting of an alternating sequence part and a Gold code (pseudo-noise [PN]) sequence part. The ratio of both sequence parts in a VDES time slot of $T_{\text{seq}} = 26.67$ ms is determined by the ranging sequence ratio $\gamma \in [0; 1]$

by the navigation data and is determined by the ranging sequence ratio $\gamma \in [0; 1]$. Figure 2 shows an example of two combined sequences utilizing a VDES time slot. Figure 3 shows the ranging sequence autocorrelation function versus the normalized time delay for different ranging sequence ratios γ . The ranging sequence ratio γ shapes the autocorrelation function. A low γ attenuates the sidelobes of the autocorrelation function to reduce the impact of ambiguity. Increasing γ sharpens the main lobe to improve the accuracy of time estimation, but on the cost of higher sidelobe levels.

In literature,¹⁰ IALA has defined accuracy requirements for a backup navigation system for GNSS considering the IMO resolution.¹⁹ The considered accuracy requirements and maximum errors causing the system to alert are listed in Table 1.

4 | THEORETICAL ASSESSMENT

In this section, we address VDES R-Mode performance aspects from estimation theory point of view. We start with considering range estimation performance based on time of arrival measurements. Then, we evaluate the performance of Doppler shift estimation, which can be used to considerably improve position estimation in a dynamic scenario. Furthermore, we discuss the impact of a satellite ranging link on the VDES R-Mode positioning performance.

For these considerations, we utilize lower bounds on estimation error variances. Specifically, we consider the Cramér–Rao bound²⁰ (CRB) and the Ziv–Zakai bound²¹ (ZZB). The ZZB is a useful addition to the CRB because it takes into account the threshold effect at low signal-to-noise ratio (SNR) values, where ambiguities significantly reduce the estimation performance. The CRB does not account for such ambiguities and, therefore, is loose in low SNR regions. We also introduce the system model for a Kalman filter that we use to process experimental measurement data in Section 5. For all these considerations, we assume that the receiver has a sufficiently accurate clock. While a practical implementation of an R-Mode receiver would not be able to use an atomic clock due to the associated costs, the effects of the clock errors are out of scope for this paper.

4.1 | Range estimation

Because VDES R-Mode is based on multilateration, it is necessary to estimate the ranges between the receiver and several BSs. This is done by estimating the time of arrival of a signal sent from the BS with a known time of transmission. Thus, the performance of the time of arrival estimator is important to the overall accuracy of the VDES R-Mode system.

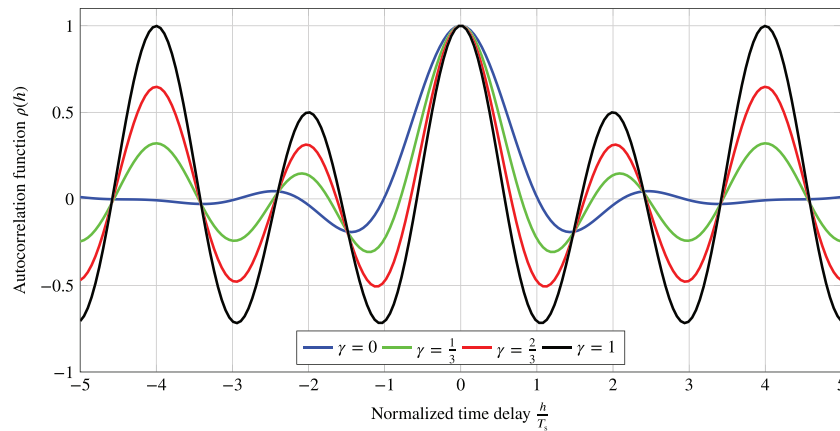


FIGURE 3 Normalized autocorrelation function $\rho(h)$ for the proposed VDES R-Mode sequences for different values of parameter γ versus time delay h , normalized to the symbol duration T_{sym}

TABLE 1 Suggested minimum accuracy requirements based on reference¹⁰ for a Global Navigation Satellite System backup system

Region	Horizontal accuracy (m)	Alert limit (m)
Ocean	1000	2500
Coastal	100	250
Port	10	25
Inland waterways	10	25

In order to evaluate this performance, we consider a signal at the receiver that can be modeled as a time delayed version of the transmitted signal corrupted by additive white Gaussian noise. In this paper, we assume that the clocks at the BS and the receiver are synchronized. Under these conditions, the received signal can be modeled as

$$x(t) = s(t - \tau) + w(t), \quad (1)$$

where $s(t)$ is the transmitted signal and $w(t)$ is the additive white Gaussian noise with a noise power spectral density of N_0 . We are interested in estimating the parameter τ , which is the delay between the transmission of the signal and its arrival at the receiver. Together with the propagation speed c_0 of the signal, an estimation

$$\hat{r} = c_0 \cdot \hat{\tau} \quad (2)$$

for the distance between transmitter and receiver, that is, the range r , can then easily be calculated from a time estimate $\hat{\tau}$.

The first bound that we consider is the CRB. For the given problem of estimating the time of arrival of a ranging signal, the CRB for an unbiased estimator states that²⁰

$$\text{var}(\hat{r}) = c_0^2 \text{var}(\hat{\tau}) \geq \frac{c_0^2}{8\pi^2 \frac{E_s}{N_0} \bar{F}^2}, \quad (3)$$

where $\text{var}(\hat{r})$ denotes the variance of the range estimate \hat{r} , $E_s = \int_{-\infty}^{\infty} |s(t)|^2 dt = \int_{-\infty}^{\infty} |S(F)|^2 dF$ is the energy of the ranging signal, N_0 is the noise power density, and

$$\bar{F}^2 = \frac{\int_{-\infty}^{\infty} F^2 |S(F)|^2 dF}{\int_{-\infty}^{\infty} |S(F)|^2 dF} \quad (4)$$

is mean square bandwidth of the signal.²⁰ This indicates that an important signal parameter for range estimation is its bandwidth. So according to the CRB, the signal's energy should be located at the edges of the available spectrum for maximizing ranging performance.

For a given signal, the CRB is often a fairly good indicator for achievable estimation performance at sufficiently high SNRs. At low SNR values, however, the achievable estimation performance is usually much lower than indicated by the CRB. Up to a certain SNR value, reliable range estimation is hard to achieve. This is known as the threshold effect. To take this phenomenon into account, we also consider the ZZB, which, unlike the CRB, takes this phenomenon into account. The ZZB is based on a comparison of the estimation problem with a detection problem.

The ZZB for time of arrival estimation is given by²¹

$$\text{var}(\hat{r}) = c_0^2 \text{var}(\hat{\tau}) \geq c_0^2 \int_0^T h \cdot \left(1 - \frac{h}{T}\right) \cdot P_e(h) dh, \quad (5)$$

where the integration interval $[0, T]$ represents an a priori time interval, within which τ is assumed to be uniformly distributed, and $P_e(h)$ is the error probability of an optimal detector deciding between the two signal hypotheses $s(t)$ and $s(t - h)$. This probability can be expressed by

$$P_e(h) = Q\left(\sqrt{\frac{E_s}{2N_0}(1 - \text{real}(\rho(h)))}\right), \quad (6)$$

where $\rho(h)$ is the autocorrelation function of signal $s(t)$, normalized to the signal's energy E_s and given by

$$\rho(h) = \frac{1}{E_s} \int_{-\infty}^{\infty} s(t) s^*(t - h) dt. \quad (7)$$

The Q-function is defined as $Q(x) = 1/\sqrt{2\pi} \int_x^{\infty} e^{-u^2/2} du$.

To calculate the ZZB according to Equation (5) of this kind of signal, we need to determine its normalized autocorrelation function according to Equation (7). This can be achieved by creating a sampled representation of the signal $s[n] = s(nT_s)$ with a sufficiently high sampling rate $f_s = 1/T_s$. Calculating its discrete autocorrelation function

$$\rho[k] = \frac{1}{E_s} \sum_n s[n] s^*[n-k] \quad (8)$$

and interpolating the discrete values by convolution with a sinc function results in a continuous autocorrelation function again:

$$\rho(h) = \sum_k \rho[k] \text{sinc}\left(\frac{h}{T_s} - k\right). \quad (9)$$

The sinc function is defined as $\text{sinc}(t) = \sin(\pi t)/\pi t$. As the autocorrelation function is practically bandlimited, this gives a very close approximation of the actual autocorrelation function. It is also easily evaluated by numerical methods.

Because the modulation parameters such as the symbol duration and the root-raised cosine roll-of factor β are given by the VDES standard, the only remaining parameters to optimize the ranging performance are the transmitted data symbols themselves. In Wirsing et al,²² we investigated the performance of different possible ranging sequences. We have found that a tradeoff needs to be made between performance at high SNRs and performance at low SNRs. A narrow autocorrelation main lobe comes with high sidelobes that cause ambiguity. In contrast, an autocorrelation function with low sidelobes shows a wider main lobe. In order to trade off between the contrary autocorrelation function's properties "main lobe steepness" and "sidelobe level," we suggested to use a concatenation of a Gold code and an alternating signal as shown in Figure 2, with the ranging sequence ratio γ^{22} as a ranging signal parameter. The influence of parameter γ on the autocorrelation function is shown in Figure 3, where we can observe that steeper main lobes result in higher sidelobe levels.

Figure 4 shows the ZZB for range estimation standard deviation for a signal with $\gamma = 1/3$ and corresponding simulation results for an a priori integration interval of $T = 12.5T_{\text{sym}} = 162.8\mu\text{s}$. At an SNR range of 10... 15 dB, both ZZB and simulation results show the threshold effect mentioned above as a severely degrading ranging performance.

4.2 | Velocity estimation

In addition to the distance between the transmitter and the receiver, it is possible to determine the radial velocity v_r as well by taking the Doppler effect into account. Due to the radial velocity between transmitter and receiver, a Doppler shift

$$\Delta f = -\frac{v_r}{c_0} f_0 \quad (10)$$

is observed at the receiver side. Note that a positive radial velocity results from an increasing transmitter–receiver distance and causes a negative Doppler shift. The ZZB for Doppler frequency estimation can be derived in a similar way to the ZZB for TOA estimation. The time domain autocorrelation function that was needed for the TOA case needs to be replaced by a frequency domain autocorrelation function

$$\rho(\Delta f) = \frac{1}{E_s} \int_{-\infty}^{\infty} S(f) S^*(f - \Delta f) df, \quad (11)$$

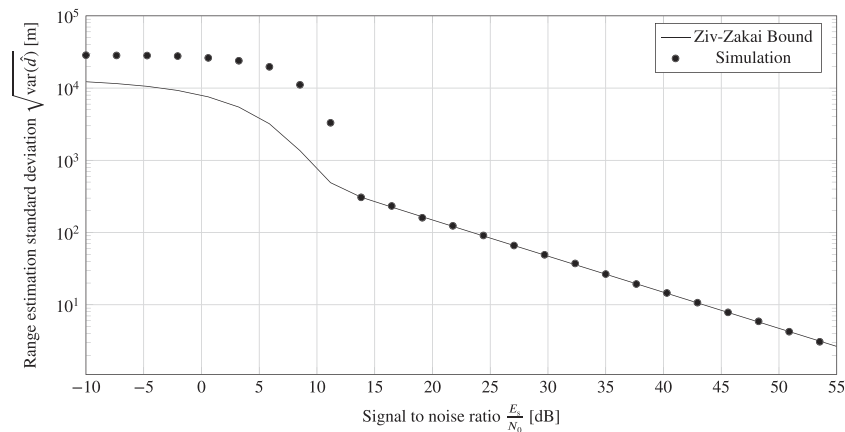


FIGURE 4 Ziv-Zakai bound for TOA-based range estimation

or equivalently by

$$\rho(\Delta f) = \frac{1}{E_s} \int_{-\infty}^{\infty} |s(t)|^2 \cdot e^{j2\pi\Delta f t} dt, \quad (12)$$

using Fourier transformation properties. If we consider a sampled representation $s(kT_s)$ of the signal, Equation (12) can be rewritten as

$$\rho(\Delta f) = \frac{\sum_k |s(kT_s)|^2 \cdot e^{j2\pi\Delta f kT_s}}{\sum_k |s(kT_s)|^2}, \quad (13)$$

which can be evaluated by numerical means. The ZZB for velocity estimation is given by

$$\text{var}(\hat{v}_r) = \left(\frac{c_0}{f_0}\right)^2 \text{var}(\Delta \hat{f}) \geq \left(\frac{c_0}{f_0}\right)^2 \int_0^{f_{\max}} \Delta f \cdot \left(1 - \frac{\Delta f}{f_{\max}}\right) \cdot Q\left(\sqrt{\frac{E_s}{2N_0}(1 - \text{real}(\rho(\Delta f)))}\right) d\Delta f, \quad (14)$$

where $\text{var}(\hat{v}_r)$ denotes the variance of the velocity estimate \hat{v}_r and the integration interval $[0, f_{\max}]$ represents an a priori frequency interval, within which Δf is assumed to be uniformly distributed. The ZZB according to Equation (14) and corresponding simulation results are shown in Figure 5 for an a priori interval of $f_{\max} = 100\text{Hz}$. Compared with the results in Figure 4, the threshold effect is less pronounced because the autocorrelation function given by Equation (11) exhibits lower sidelobes than the time domain ranging signal autocorrelation function.

4.3 | On satellite links in VDES R-Mode positioning

In this section, we aim to evaluate the achievable gain in VDES R-Mode positioning performance when including a satellite ranging link. For this purpose, we consider a scenario, where VDES R-Mode BSs are located along a coastline. Such a BS arrangement provides a poor geometry, that is, providing high dilution of precision (DOP) values, at areas close to the coastline. In those coastline areas, the position estimation performance in particular suffers from a high uncertainty in the direction perpendicular to the coastline. A satellite ranging link can improve the poor DOP performance from geometry point of view. However, compared with terrestrial VDES R-Mode ranging links, a satellite ranging link provides a lower transmit power and, at the same time, significantly higher signal propagation loss due to the much higher distance between the satellite and receiver. This leads to a much lower ranging SNR and, consequently, to a higher ranging variance for the satellite link compared with the terrestrial VDES ranging links. Therefore, in order to assess the benefit of a satellite link in VDES R-Mode positioning, it is not sufficient to consider the DOP only. Instead, we evaluate the positioning CRB, which accounts for different range link performances in addition to geometry.

As an exemplary setup, we consider two VDES R-Mode BSs located at the positions $\mathbf{p}_1 = [x_1, y_1, z_1] = [-10\text{km}, 0, 150\text{m}]$ and $\mathbf{p}_2 = [+10\text{km}, 0, 150\text{m}]$ along a coastline ($x, y = 0, z = 0$) in Cartesian coordinates. With this setting, we assume a TX antenna height of $h_{\text{TX}} = 150\text{m}$ above sea level $z = 0$. An additional satellite is located at $\mathbf{p}_3 = [0, 2000\text{km}, \tan(\theta) \cdot 2000\text{km}]$ at an elevation of $\theta = 10^\circ$. The receiver (RX) antenna is

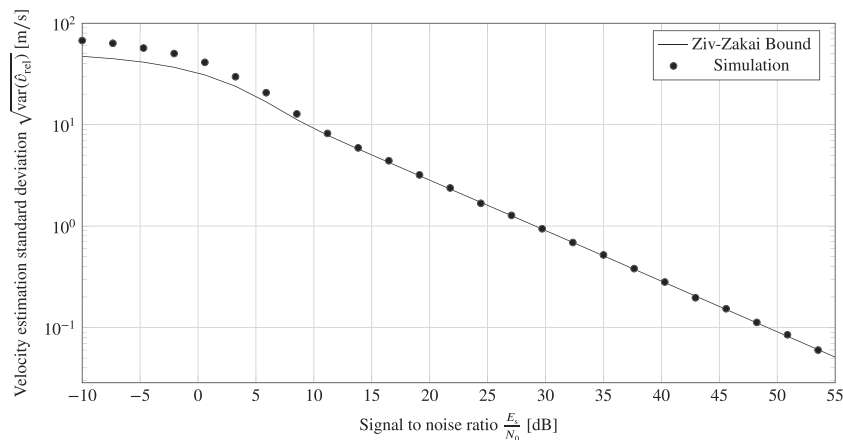


FIGURE 5 Ziv-Zakai bound for Doppler-based velocity estimation

located at position $\mathbf{p} = [x, y, z = 10\text{m}]$, so we face a two-dimensional estimation problem with unknown coordinates x and y . For our first evaluations, we assume that transmitters (TXs) and the RX are synchronized in time. We start with the calculation of the different ranging signal power levels

$$P_{RXn} = \frac{P_{EIRPn}}{L_n} G_{RX} \quad (15)$$

that occur at the RX. The RX power depends on the effective isotropic radiated power (EIRP) P_{EIRPn} of the ranging signals, which are transmitted at TX positions \mathbf{p}_n . Note that P_{EIRPn} already takes into account a TX antenna gain. G_{RX} is the RX antenna gain. L_n denotes the signal propagation path loss between the TX at position \mathbf{p}_n and the RX. The path loss L_n is strongly dependent on the distance $d_n = |\mathbf{p}_n - \mathbf{p}| = \sqrt{(x_n - x)^2 + (y_n - y)^2 + (z_n - z)^2}$ between TX and RX. Environmental conditions around and between TX and RX also influence the signal propagation conditions and, therefore, the path loss. To account for the terrestrial signal propagation from VDES R-Mode BSs over sea to the RX, we apply an appropriate path loss model proposed in Recommendation ITU-R P.1546-6.²³ Figure 6 shows the corresponding path loss versus the horizontal distance $r_n = \sqrt{(x_n - x)^2 + (y_n - y)^2}$ between TX and RX for a carrier frequency of $f_c = 160\text{MHz}$, RX antenna height $h_{RX} = 10\text{m}$, and different TX antenna heights h_{TX} . The graphs represent path loss values that are undercut at 50% of the locations and for 50% of the time for sea paths. As a comparison, the free space path loss is shown for equal TX and RX antenna heights, here $h_{TX} = h_{RX} = 10\text{m}$. For simulation, we have used the path loss model for a TX antenna height of $h_{TX} = 150\text{m}$.

For the link between satellite and RX, we assume unobstructed signal propagation and, therefore, free space signal propagation with path loss

$$L_n = \left(\frac{4\pi f_c d_n}{c_0} \right)^2 \quad (16)$$

for carrier frequency f_c , speed of light c_0 , and with d_n as the distance between TX and RX. From the ranging signal power levels P_{RXn} , we obtain the corresponding VDES R-Mode ranging SNRs

$$\left(\frac{E_s}{N_0} \right)_n = \frac{P_{RXn} T_{\text{seq}}}{k_B T_{\text{noise}} F}, \quad n = 1, 2, 3, \quad (17)$$

with ranging signal duration T_{seq} , receiver noise temperature T_{noise} , receiver noise figure F , and Boltzmann constant k_B . Applying these SNRs to Equation (3), we obtain the ranging CRBs

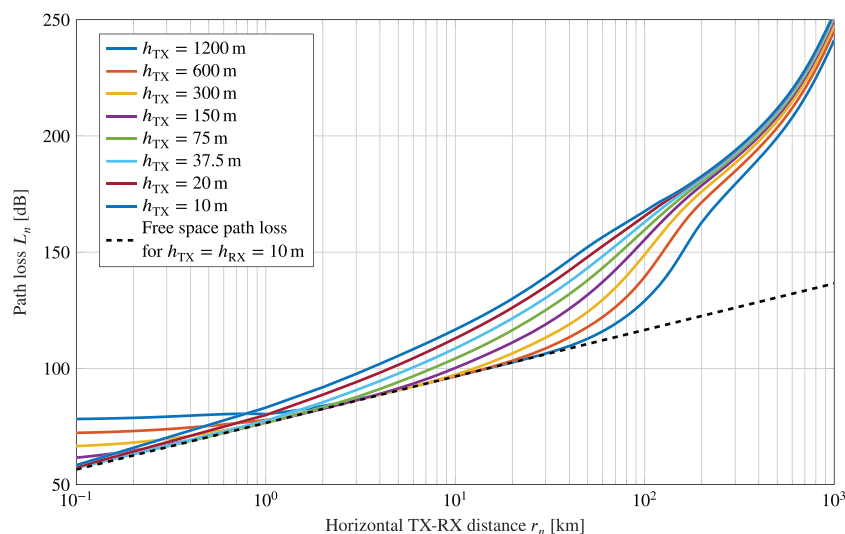


FIGURE 6 Signal propagation path loss between VDES R-Mode BSs and the RX according to Recommendation ITU-R P.1546-6²³ for a carrier frequency of $f_c = 160\text{MHz}$, RX antenna height $h_{RX} = 10\text{m}$, and different TX antenna heights h_{TX} . The graphs represent path loss values that are undercut at 50% of the locations and for 50% of the time for sea paths. As a comparison, the free space path loss is shown for equal TX and RX antenna heights, here $h_{TX} = h_{RX} = 10\text{m}$. For simulation, we use $h_{TX} = 150\text{m}$

$$\sigma_n^2 = \frac{c_0^2}{8\pi^2 \left(\frac{E_s}{N_0}\right)_n F^2}, \quad n = 1, 2, 3. \quad (18)$$

We choose a VDES R-Mode signal bandwidth of $B = 100$ kHz for terrestrial links and $B = 150$ kHz for satellite links. Assuming a uniform power spectrum density yields, according to Equation (4), a mean square bandwidth of

$$\bar{F}^2 = \frac{B^2}{12}. \quad (19)$$

Table 2 summarizes the system parameters that we have used for simulation.

We collect the ranging CRBs, which we get from Equation (18) in a diagonal matrix $\Sigma = \text{diag}(\sigma_1^2, \sigma_2^2, \sigma_3^2)$ and define the Jacobian matrix

$$\mathbf{J} = \begin{pmatrix} \frac{\partial}{\partial x} d_1 & \frac{\partial}{\partial y} d_1 \\ \frac{\partial}{\partial x} d_2 & \frac{\partial}{\partial y} d_2 \\ \frac{\partial}{\partial x} d_3 & \frac{\partial}{\partial y} d_3 \end{pmatrix}, \quad (20)$$

where d_i denote the distance between TX n at position $\mathbf{p}_n = [x_n, y_n, z_n]$ and the RX at position $\mathbf{p} = [x, y, z = 10\text{m}]$. With these definitions, we calculate the Fisher information matrix^{20,24}

$$\mathbf{FIM} = \mathbf{J}^T \Sigma^{-1} \mathbf{J} \quad (21)$$

as well as the corresponding CRB matrix

$$\mathbf{CRB} = \mathbf{FIM}^{-1} \quad (22)$$

for two-dimensional position estimation. The diagonal elements of **CRB** describe the corresponding CRBs, that is, the lower bounds on the variances of the estimates \hat{x} and \hat{y} of the receivers position coordinates in the $(x, y, z = 10\text{m})$ plane. We obtain the positioning CRB as

$$\sigma_{\text{pos}} = \sqrt{\text{tr}(\mathbf{CRB})} \quad (23)$$

as the square root of the trace of the CRB matrix calculated from Equation (22).

TABLE 2 VDES R-Mode simulation parameters

Parameter		Value
Carrier frequency	f_c	160 MHz
Mean VDES R-Mode TX power (EIRP)	P_{EIRP}	12.5 W (VDES terrestrial) 1 W (VDES satellite)
VDES R-Mode signal bandwidth	B	100 kHz (VDES terrestrial) 150 kHz (VDES satellite)
VDES R-Mode signal duration	T_{seq}	26.67 ms (VDES terrestrial) $15 \times 26.67 \text{ ms} = 400 \text{ ms}$ (VDES satellite)
Receiver antenna gain	G_{RX}	1 (0 dB)
Receiver noise power spectral density	N_0	$N_0 = k_B T_{\text{noise}}$
Receiver noise temperature	T_{noise}	300 K
Receiver noise figure	F	5 (7 dB)
Boltzmann constant	k_B	$1.381 \cdot 10^{-23}$ J/K
Speed of light	c_0	299 792 458 m/s

We start our discussion with considering terrestrial VDES R-Mode position estimation, where we observe ranging signals from terrestrial BS located at $\mathbf{p}_1 = [x_1, y_1, z_1] = [-10\text{km}, 0, 150\text{m}]$ and $\mathbf{p}_2 = [+10\text{km}, 0, 150\text{m}]$. From Figure 7A, we observe that the best positioning performance can be obtained at distances of 5...10km apart from the coastline. When approaching the coastline, the positioning performance decreases despite increasing ranging signal SNRs. For a clearer view on the coastline area, Figure 7C shows a logarithmic zoom of Figure 7A in y -direction. The reason for this performance degradation is the influence of the poor geometry, accounted by the DOP. In particular, the position estimation variance for the y -coordinate increases drastically when approaching the coastline. Note, for the calculation of this CRB, we do not consider a satellite ranging link. We can account for this by using the upper left 2×2 submatrix of the Fisher information matrix definition, shown in Equation (21), when calculating the CRB matrix \mathbf{CRB} according to Equation (22).

Now, let us include a third TX on a satellite located at $\mathbf{p}_3 = [0, 2000\text{km}, \tan(\theta) \cdot 2000\text{km}]$ at an elevation of $\theta = 10^\circ$. From Figure 7B,D, we observe that the positioning performance is noticeably improved in areas close to the coastline. Figure 8 shows the ratio of the CRB for positioning with two BSs plus one satellite and the CRB for positioning with two BSs only. That is, this figure shows the result shown in Figure 7D divided by those shown in Figure 7C. With increasing distance to the coastline, the performance gain becomes more and more negligible. We also observe that very close to the coastline the performance improvements are in the order of up to 2 orders of magnitude. However, the absolute positioning error when including a satellite ranging link is still at a tremendously high level in this region as Figure 7D shows. The reason for remaining at high positioning errors when including a satellite ranging link is the high ranging variance of the satellite link. The satellite link's ranging CRB is in the order of a few thousand meters for the parameter setting we have used. Thus, we can expect to observe VDES R-Mode positioning performance improvements due to the satellite link only in regions where the positioning performance with terrestrial links is also in the order of a few thousand meters and, in addition, the satellite link improves the DOP.

Improving the satellite ranging performance requires to increase the received ranging signal energy by increasing the EIRP and/or the ranging signal duration. Another opportunity for increasing ranging performance is to increase the satellite's ranging signal bandwidth.

4.4 | Position estimation and tracking using a Kalman filter

To determine the position information, it is necessary to combine multiple range measurements into one position estimate. For the range estimates, as described in Section 4.1, this can be done on a snapshot basis for each individual set of measurements. In order to utilize the radial velocities, as described in Section 4.2, it is necessary to consider the receiver as a dynamic system.

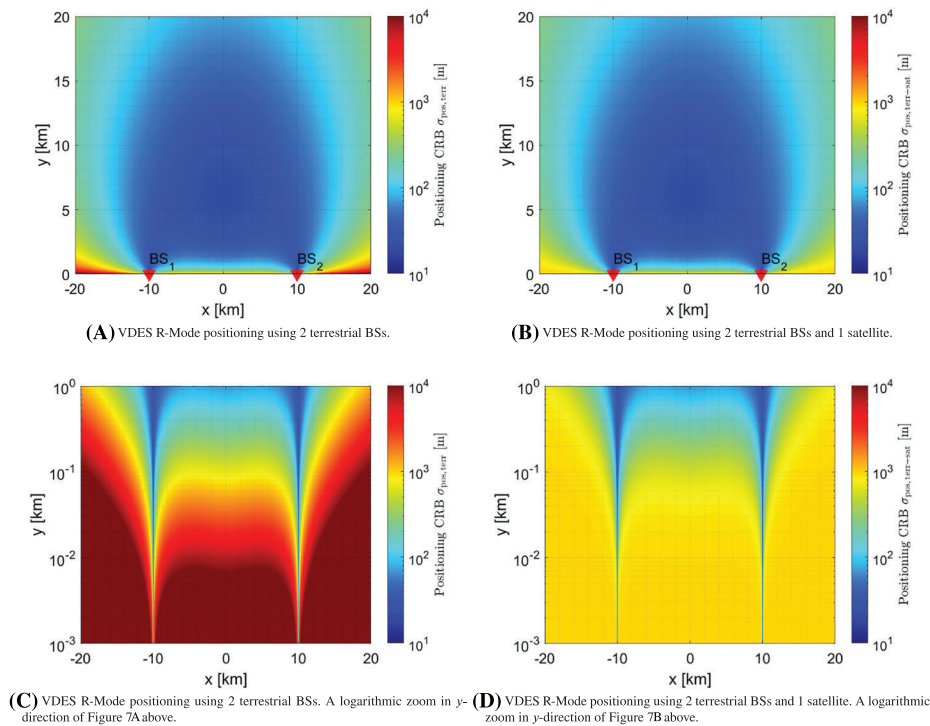


FIGURE 7 Cramér–Rao bounds for VDES R-Mode position estimation in a two-dimensional plane ($x, y, z = 10\text{m}$)

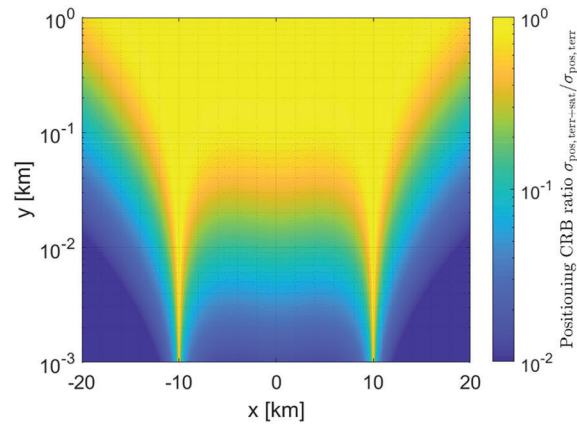


FIGURE 8 Ratio of the CRB for positioning with two BSs plus one satellite and the CRB for positioning with two BSs only. That is, this figure shows the result shown in Figure 7D divided by those shown in Figure 7C

A good tool to use for estimating the state of a dynamic system is the Kalman filter.²⁵ The unmodified Kalman filter is applicable for linear systems only. The positioning problem though is nonlinear because the measured ranges and radial velocities cannot be expressed as a linear function of the receiver position. For this reason, we use an unscented Kalman filter (UKF), which is applicable to nonlinear problems as well.²⁶ The general working principle of a Kalman filter as well as a description of the unscented transform, which is the basis of the UKF, can be found in the literature.^{25,26}

Thus, in this paper, we present the UKF implementation, specific to the R-Mode system. The state vector that we use for the UKF is

$$\mathbf{x} = \begin{pmatrix} x \\ y \\ v_x \\ v_y \\ a_x \\ a_y \end{pmatrix}. \quad (24)$$

It contains the 2D position consisting of x and y in a local Cartesian coordinate system, as well as 2D velocity and acceleration. The height is not considered because we're dealing with a maritime system and the receiver is assumed to be at a constant height above the water. The clock bias and drift are also not considered here; however, they would need to be tracked as well for a practical implementation where the receiver does not have a highly accurate clock. The dynamics of the boat are modeled by a simple constant acceleration model, given by the differential equation

$$\frac{d}{dt}\mathbf{x} = \mathbf{A}\mathbf{x} \quad (25)$$

with

$$\mathbf{A} = \begin{pmatrix} 0 & 0 & 1 & 0 & 0 & 0 \\ 0 & 0 & 0 & 1 & 0 & 0 \\ 0 & 0 & 0 & 0 & 1 & 0 \\ 0 & 0 & 0 & 0 & 0 & 1 \\ 0 & 0 & 0 & 0 & 0 & 0 \\ 0 & 0 & 0 & 0 & 0 & 0 \end{pmatrix}. \quad (26)$$

The state transition matrix is then given by

$$\mathbf{F} = e^{\Delta t \mathbf{A}} = \begin{pmatrix} 1 & 0 & \Delta t & 0 & \frac{\Delta t^2}{2} & 0 \\ 0 & 1 & 0 & \Delta t & 0 & \frac{\Delta t^2}{2} \\ 0 & 0 & 1 & 0 & \Delta t & 0 \\ 0 & 0 & 0 & 1 & 0 & \Delta t \\ 0 & 0 & 0 & 0 & 1 & 0 \\ 0 & 0 & 0 & 0 & 0 & 1 \end{pmatrix}, \quad (27)$$

where Δt is the time difference between the state updates. The system noise covariance matrix \mathbf{Q} is assumed to be

$$\mathbf{Q} = q \begin{pmatrix} \frac{\Delta t^5}{20} & 0 & \frac{\Delta t^4}{8} & 0 & \frac{\Delta t^3}{6} & 0 \\ 0 & \frac{\Delta t^5}{20} & 0 & \frac{\Delta t^4}{8} & 0 & \frac{\Delta t^3}{6} \\ \frac{\Delta t^4}{8} & 0 & \frac{\Delta t^3}{3} & 0 & \frac{\Delta t^2}{2} & 0 \\ 0 & \frac{\Delta t^4}{8} & 0 & \frac{\Delta t^3}{3} & 0 & \frac{\Delta t^2}{2} \\ \frac{\Delta t^3}{6} & 0 & \frac{\Delta t^2}{2} & 0 & \Delta t & 0 \\ 0 & \frac{\Delta t^3}{6} & 0 & \frac{\Delta t^2}{2} & 0 & \Delta t \end{pmatrix}, \quad (28)$$

which corresponds to a white noise with variance q that only affects the acceleration of the receiver. The UKF allows to update the current position estimate with each new observation of a signal that is received from VDES R-Mode BSs. As the velocity of the ship is tracked in the UKF, it is easy to incorporate the measurements of the radial velocities into the evaluation. The observation vector \mathbf{z} consists of the ranges r_n and the radial velocities $v_{r,n}$ to the respective BSs:

$$\mathbf{z} = \begin{pmatrix} r_1 \\ \vdots \\ r_N \\ v_{r,1} \\ \vdots \\ v_{r,N} \end{pmatrix}. \quad (29)$$

The expected observations \mathbf{z} depending on the state vector \mathbf{x} can be expressed by the nonlinear expressions

$$r_n = \sqrt{(x - x_n)^2 + (y - y_n)^2} \quad (30)$$

$$v_{r,n} = \frac{v_x(x - x_n) + v_y(y - y_n)}{r_n} \quad (31)$$

with $n = 1, \dots, N$, where r_n and $v_{r,n}$ represent the range and radial velocity with respect to the n th BS and x_n together with y_n represents the position of that BS.

Using a UKF allows us to utilize the Doppler measurements to track the ship's position. Notably, if a good estimate of the ship's velocity is known, such as tracked from a previous measurement, the radial velocity as defined in Equation (31) still depends on the position and thus can be used for position estimates. Especially for small distances r_n , this effect is considerable. The computational complexity of the UKF is also suitable for real-time tracking.

5 | MEASUREMENTS

In order to test the practical implementation of a VDES R-Mode system, we performed and assessed measurements on Lake Ammer near Munich in Bavaria. These measurements were the first experimental results of VDES R-Mode that resulted in a successfully estimated position. The

measurement setup consisted of three land-based stations that transmitted a VDES R-Mode ranging signal as defined in literature² and a mobile transceiver unit that was placed on a boat.

5.1 | Measurement setup

The land side of the measurement setup consisted of three temporarily erected masts that were located on the shore of Lake Ammer, with the antennas at a height of approximately 10 m above the water. Each of the transmitters consisted of a laptop, a USRP B210 software defined radio, an amplifier, and a Septentrio PolaRx5TR GNSS receiver. The GNSS receiver was used to provide precise position information and accurate timing information to each of the BSs. The setup of one of the land stations can be seen in Figure 9A.

To coordinate the transmissions of different BSs, each BS was assigned a specific time slot, relative to the full second following the Media Access Control (MAC) layer allocation defined in the VDES standard.¹⁶ While the intended transmit power of a VDES BS, according to the standard, is 12.5 W without antenna gain, we were limited to a transmit power of 1-W EIRP based on the license of the German regulatory agency. Due to the use of a TX/RX switch, each of the land stations was also able to receive while not transmitting.

The positions of the transmitters were chosen in a way that sets up a good geometry for positioning estimation in the northern part of Lake Ammer. Specifically, the three transmitters were located at the waterside of the villages Utting, Buch, and Schondorf. Their location and the outline of the lake can be seen in Figure 13.

The mobile setup was similar to the setup of the land stations. Because the land stations are able to receive outside of their assigned transmit time slot, the mobile station was assigned a transmit time slot, too. However, this data set is foreseen for future evaluations. Like the land-based stations, the mobile station was equipped with a GNSS receiver to provide precise position information as reference and an accurate timing signal for the SDR. This is a deviation from the R-Mode system design that envisages clocks with lower accuracy at the receiver. However, investigating the effects of a less accurate clock was not in the scope of this experiment.

The Wasserwacht Bayern (water rescue Bavaria) supported us by driving our mobile station with a motorized boat. The antenna setup on the boat is shown in Figure 9B.

As VDES only provides a single 100-kHz channel, it was not possible to assign each transmitter its own frequency. Thus, a time multiplexed setup was chosen. Each transmitter was assigned a 250-ms time slot, within which it could transmit without interference from the other transmitters. Figure 10 illustrates this approach.

5.2 | Measurement results

The setup during the measurement was recording all data samples. The data evaluation itself was done in postprocessing. In order to obtain estimates for the ranges and for the radial velocities, a maximum likelihood approach was used. This means that the delay τ and the Doppler shift Δf were estimated by

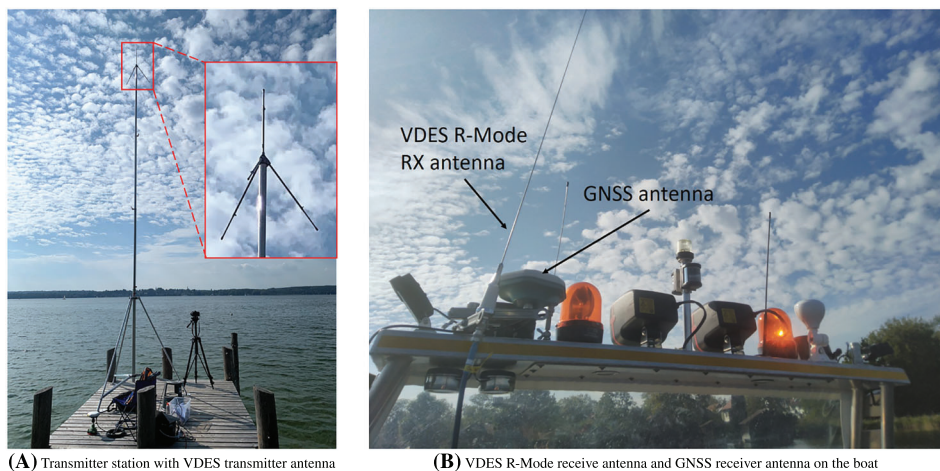


FIGURE 9 Transmitter and receiver setup at Lake Ammer

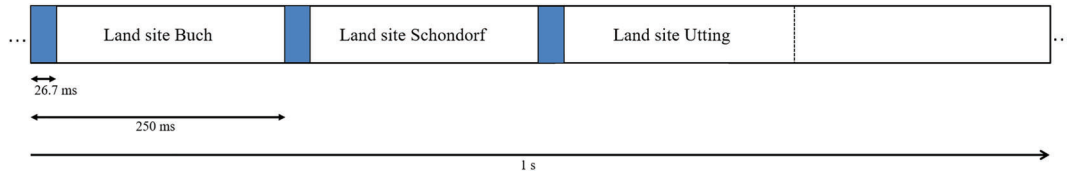


FIGURE 10 Time scheduling of the different land transmitters. The blue colored area represents the ranging sequence of length $T_{\text{seq}} = 26.67\text{ms}$ or one VDE time slot

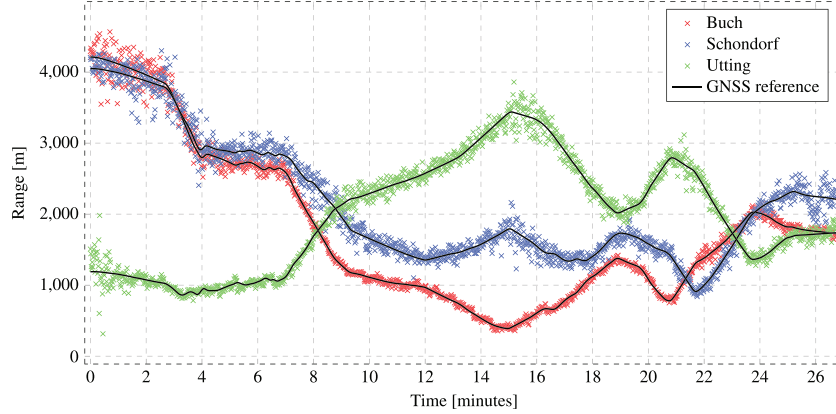


FIGURE 11 Estimated ranges and the Global Navigation Satellite System (GNSS) reference

$$(\hat{\tau}, \Delta\hat{f}) = \arg \max_{\tau, \Delta f} \sum_k x[k] \cdot s^*(kT_s - \tau) e^{j2\pi k T_s \Delta f} \quad (32)$$

with $x[k]$ being the received samples from the USRP and $s(t)$ being the transmitted signal. A numerical optimizer was used to evaluate the argmax operation. Because the signal delay from the SDR was not calibrated, all of the range measurements had a constant offset and the range estimate \hat{r} was obtained as

$$\hat{r} = c_0 \cdot (\hat{\tau} - \tau_{\text{offset}}). \quad (33)$$

The offset parameter τ_{offset} was obtained by comparing the estimated values with reference values from the GNSS receiver. The range measurements obtained this way are shown in Figure 11 for each BS, along with the corresponding reference values from the GNSS receiver.

For the Doppler frequency-based estimation of the radial velocity, no such measures were necessary. The estimate for the radial velocity \hat{v}_r was easily obtainable by

$$\hat{v}_r = -\Delta\hat{f} \frac{c_0}{f_0}. \quad (34)$$

The estimated velocities and their reference values are shown in Figure 12. Each plot shows the estimated values for all three BSs, as well as the reference values obtained from the GNSS data.

We implemented a UKF in Matlab, as described in Section 4.4, in order to track the boat's position and the boat's velocity. This tracking was done in a local Cartesian coordinate system. The zero coordinate was chosen as the mean position of the three BSs. The noise parameters in the Kalman filter were determined empirically. The evaluation was performed twice: once with only the range measurements and once with the measurements of the radial velocity in addition. The resulting estimated track of the ship for both evaluations is shown in Figure 13. The results for the estimated speed are shown in Figure 14. It can be seen in that plot that the addition of the radial velocity measurements to the evaluation significantly improved the positioning performance. To illustrate this further, the absolute difference of the tracked position to the GNSS reference position is being shown in Figure 15 for both evaluations. Figure 16 shows the empirical cumulative distribution function (CDF) of the positioning error with and without the Doppler observations under line of sight conditions. The first 5 min of the recorded data were omitted from the computation of the CDF due to the non-line of sight conditions between the boat and the Utting land station. From this plot, we can see that the

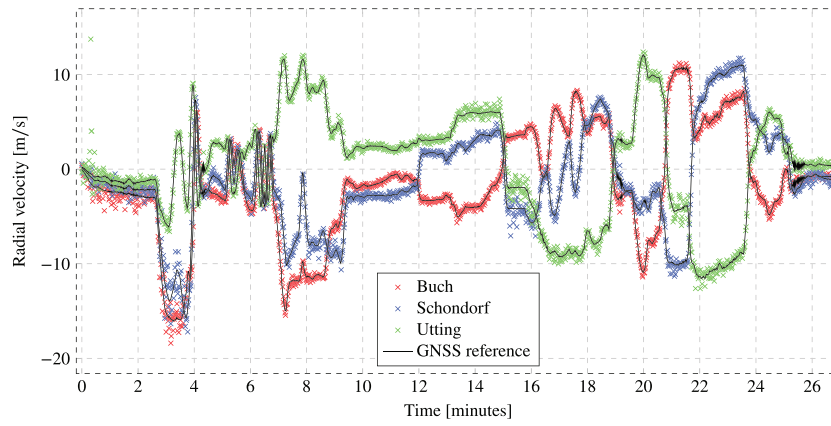


FIGURE 12 Estimated radial velocity. GNSS, Global Navigation Satellite System

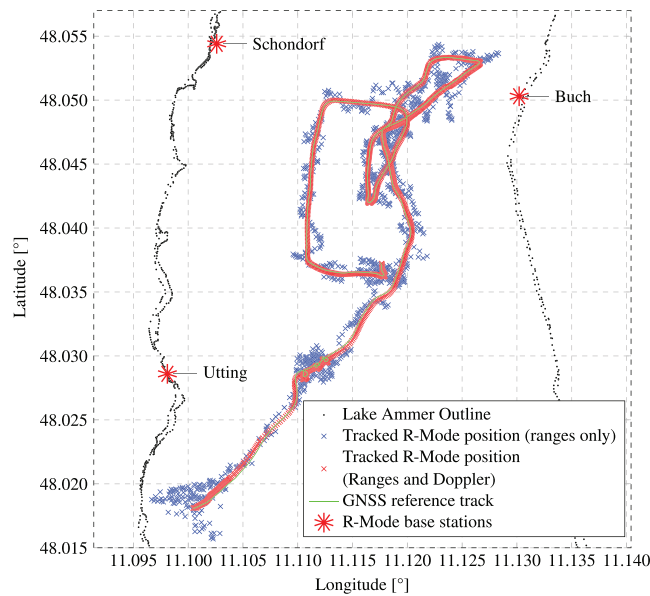


FIGURE 13 Positioning results of the Lake Ammer measurement. GNSS, Global Navigation Satellite System

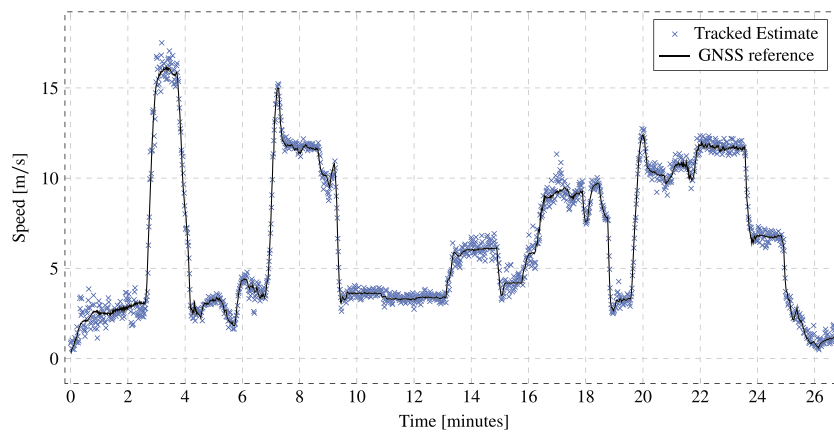


FIGURE 14 Estimated speed and reference speed obtained by Global Navigation Satellite System (GNSS)

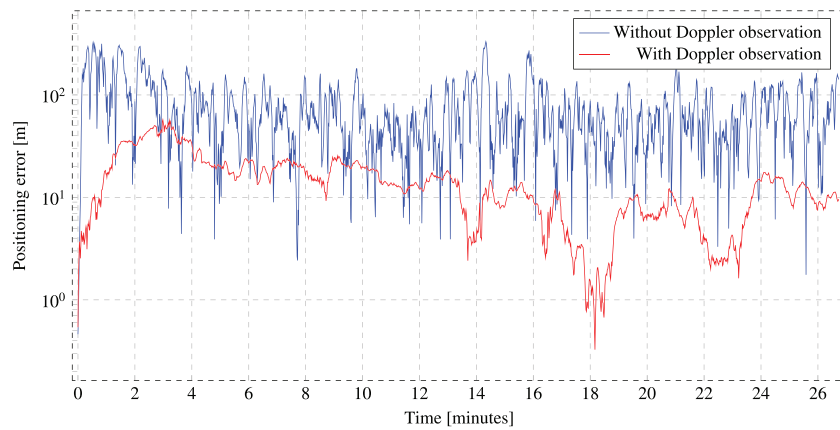


FIGURE 15 Positioning error after Kalman filtering

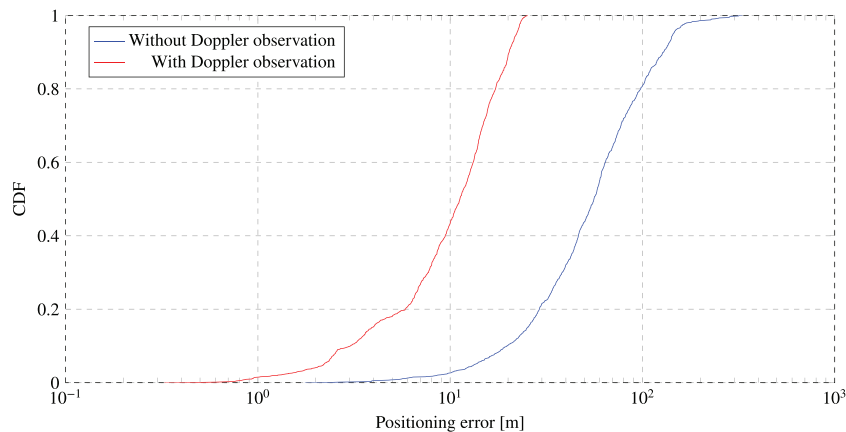


FIGURE 16 Positioning error cumulative distribution function (CDF) under line of sight conditions

positioning accuracy that was achieved 95% was 145 m without the Doppler observations, and 22 m with them. The effect of the Doppler observations on the estimated velocity is also considerable, as can be seen in Figure 17.

6 | DISCUSSION

In this section, we discuss the theoretical and practical assessment of VDES R-Mode by terrestrial and satellite VDE.

6.1 | Measurement results

The measurement results show that estimating a position by utilizing VDES R-Mode signals is possible and that an accuracy of about 10 m can be achieved under good conditions where the line of sight between transmitter and receiver is unobstructed and the geometry of the BSs corresponds to a small DOP. Our measurements took place on Lake Ammer. Due to the limited distances between the BSs and the boat, the scenario represents a situation that could occur close to the coast, such as when approaching a harbor. As the density of maritime traffic is highest close to the harbor, resulting in high requirements on the positioning, this is an important use case of the R-Mode system. Because the transmit power in our experiments was only 1 W, which is 11 dB below the 12.5 W intended by the standard, it is plausible that, using the full power, similar results can be achieved at higher distances as well.

Consistent with the theoretical considerations in Section 4, the results of the Doppler estimation in meter per second were more accurate than the ranging results in meter. While the available literature on VDES R-Mode focuses on the range estimation aspect, our experimental

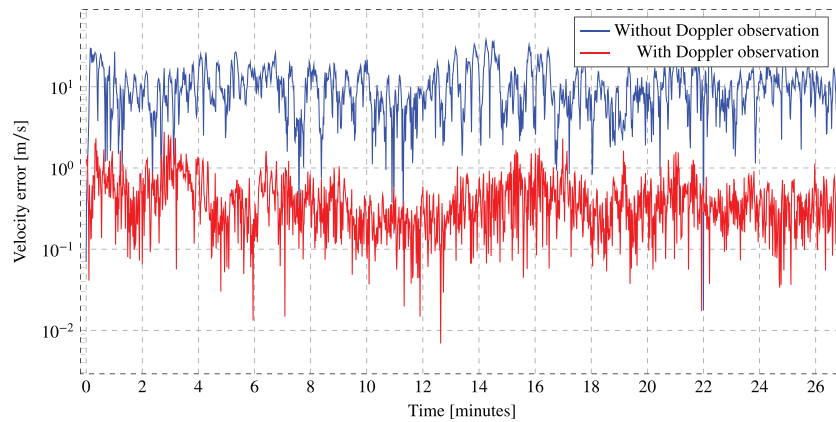


FIGURE 17 Absolute error of the estimated velocity after Kalman tracking

results show that using the Doppler shift to estimate the radial velocity of the vehicle can greatly improve the accuracy of the tracked position estimate. As described in Section 4.1, the ranging performance depends on the bandwidth of the signal. The VDE system however offers only 100-kHz bandwidth, which limits the ranging performance. In contrast to that, the Doppler estimation performance depends on the duration of the signal, which could be increased further by utilizing multiple time slots of the VDE system coherently. This approach would increase the load on the VDE system. Because VDES is primarily a communication system, any resources that are solely dedicated to R-Mode will decrease the system's capacity for data transmission. Further research of how much performance can be gained by improving the Doppler estimation should be performed.

6.2 | Using satellite links to complement terrestrial R-Mode

VDES BSs are currently in development and will most likely replace the current AIS BSs. The AIS shore network was planned to cover the sea and to avoid overlapping areas to reduce the need for interference management between BSs. For a future VDES R-Mode network, additional BSs would enable the vessel to position and track itself to complement or even be independent of GNSS.

Further, VDES satellite providers are currently assessing the performance of VDE-S for communication needs especially on the open sea. We considered utilizing the VDE-S for ranging as well. The low transmit power compared with the terrestrial VDE-T link together with the significant signal propagation distance limits the impact of the additional ranging link significantly in coastal areas. On the other side, VDE-S allows to utilize according to the IALA Guideline 1139³ between 15 and 90 consecutive time slots to transmit data that could be used as a ranging sequence. This increases the collected energy at the receiver and the SNR accordingly. In distant areas or even open sea, the performance requirements are significantly lower. Our theoretical performance assessment in Section 4.3 evaluates the performance gains and shows indeed in coastal areas the satellite link is of minor interest despite the potential improvement of the GDOP. In distant areas, the VDE-T received power drops significantly and is therefore comparable with the satellite link. A dense VDES satellite network could provide a positioning service particularly in open sea areas with no terrestrial coverage but with limited performance.

Further, such areas are still of interest as the areas are beyond the communication coverage of the terrestrial VDES network. Therefore, a dense satellite network could be of significant interest to regularly provide vessels beyond the communication coverage zones with relevant navigation data. The navigation data comprise crucial information that is relevant to position the vessel.

6.3 | Synchronization and timing in VDES R-Mode

Positioning using radio signal propagation delay methods requires sufficiently accurate timing at both the VDES R-Mode BSs and a VDES R-Mode receiver. The required precision for timing depends on the targeted positioning accuracy of VDES R-Mode. Consequently, the timing accuracy has to stay at least in the order of the targeted positioning respectively ranging accuracy divided by the speed of light. For achieving a positioning accuracy in the order of 10 m, 10-ns root mean square (RMS) for mutual timing errors between BSs have been budgeted in Rieck et al.²⁷ Also in Rieck et al.,²⁷ several options for providing sufficiently accurate synchronization and timing for VDES R-Mode are discussed, where the authors conclude that a self-synchronization approach, using R-Mode signals in the MF or VHF bands in combination with sufficiently stable local clocks, has the potential to make R-Mode a self-contained alternative positioning system for GNSS.

7 | CONCLUSIONS AND OUTLOOK

In this paper, we have addressed system design aspects and evaluated the positioning performance of VDES R-Mode. The VDES R-Mode positioning performance has been evaluated using both estimation theoretic and experimental methods. Using Fisher information theory, we have investigated the potential benefit of a VDES satellite ranging link to R-Mode. It has been found that such a satellite ranging link does not provide sufficient performance improvements due to low observed signal power levels. VDES satellites, however, can still be an important part of the R-Mode system by distributing the required navigation information.

For evaluation and validation of VDES R-Mode, we have described an experiment which we conducted at Lake Ammer, southwest of Munich. Including Doppler observations, in addition to range estimates, for position and velocity tracking at the VDES R-Mode receiver improves the positioning accuracy significantly. The extent of the possible improvements should be further investigated. Our experimental results show that VDES R-Mode is capable of achieving a 95th-percentile horizontal position error of 22 m under line of sight conditions with good geometry. Thus, VDES R-Mode is a promising approach for a maritime GNSS backup system, which can fulfill the accuracy requirements of IALA, as defined in literature.¹⁰

ACKNOWLEDGMENTS

We would like to thank the staff of the Wasserwacht Utting for their valuable support during the experiment at Lake Ammer. This study was carried out within the R-Mode Baltic project, partly funded by the European Union through the European Regional Development Fund within the Interreg Baltic Sea Region Programme.

DATA AVAILABILITY STATEMENT

The data that support the findings of this study are available from the corresponding author upon reasonable request.

ORCID

Markus Wirsing  <https://orcid.org/0000-0002-7192-5831>

Armin Dammann  <https://orcid.org/0000-0002-7112-1833>

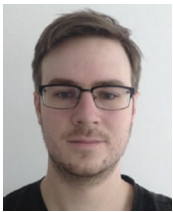
Ronald Raulefs  <https://orcid.org/0000-0002-3409-6640>

REFERENCES

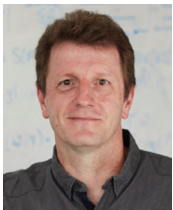
1. Volpe JA. Vulnerability Assessment of the Transportation Infrastructure Relying on the Global Positioning System. tech. rep., United States. Department of Transportation; 2001.
2. IALA Guideline G1158: VDES R-Mode ed. 1. 2020.
3. IALA Guideline G1139: THE TECHNICAL SPECIFICATION OF VDES, ed. 3. 2019.
4. Oltmann JH, Hoppe M. Contribution to the IALA World Wide Radio Navigation plan (IALA WWRNP)/Recapitalization of MF DGNS Systems. tech. rep., IALA; 2008.
5. NAV 54/25 REPORT TO THE MARITIME SAFETY COMMITTEE. tech. rep., INTERNATIONAL MARITIME ORGANIZATION (SUB-COMMITTEE ON SAFETY OF NAVIGATION); 2008.
6. Johnson G, Swaszek P. Feasibility Study of R-Mode using MF DGPS Transmissions. tech. rep., Accseas Project; 2014.
7. Johnson G, Swaszek P. Feasibility Study of R-Mode using AIS Transmissions Issue. tech. rep., Accseas Project; 2014.
8. Jiang Y, Zheng K. The Single-Shore-Station-Based Position Estimation Method of an Automatic Identification System. *Sensors*. 2020;20(6):1590. <https://doi.org/10.3390/s20061590>
9. Šafář J, Grant A, Williams P, Ward N. Performance Bounds for VDES R-mode. *J Navig*. 2020;73(1):92-114. <https://doi.org/10.1017/S0373463319000559>
10. IALA Recommendation R-129 GNSS VULNERABILITY AND MITIGATION MEASURES (Edition 3.1). 2012.
11. Sadlier G, Flytkjær R, Sabri F, Herr D. The economic impact on the UK of a disruption to GNSS. tech. rep., Innovate UK; 2017.
12. Diggelen vF. *A-GPS: Assisted GPS, GNSS, and SBAS*. Artech House; 2009.
13. del Peral-Rosado JA, Raulefs R, López-Salcedo JA, Seco-Granados G. Survey of Cellular Mobile Radio Localization Methods: From 1G to 5G. *IEEE Commun Surv Tutor*. 2018;20(2):1124-1148. <https://doi.org/10.1109/COMST.2017.2785181>
14. Koch P, Gewies S. Worldwide Availability of Maritime Medium-Frequency Radio Infrastructure for R-Mode-Supported Navigation. *J Marine Sci Eng*. 2020;8(3):209.
15. Grundhöfer L, Gewies S, Hehenkamp N, Galdo GD. Redesigned Waveforms in the Maritime Medium Frequency Bands. In: *Proceedings IEEE/ION Position, Location and Navigation Symposium (PLANS) 2020*; 2020.
16. ITU-R Recommendation M.2092: Technical Characteristics for a VHF Data Exchange System in the VHF Maritime Mobile Band 2015.
17. ITU-R Recommendation M.1371: Technical characteristics for an automatic identification system using time-division multiple access in the VHF maritime mobile band. 2014.
18. IMO Resolution MSC.401(95) PERFORMANCE STANDARDS FOR MULTI-SYSTEM SHIPBORNE RADIONAVIGATION RECEIVERS. 2015.
19. IMO Resolution A.1046(27) WORLDWIDE RADIONAVIGATION SYSTEM. 2011.
20. Kay SM. *Fundamentals of Statistical Processing, Volume I: Estimation Theory* ch. 3. Prentice Hall PTR; 1993.

21. Chazan D, Zakai M, Ziv J. Improved Lower Bounds on Signal Parameter Estimation. *IEEE Trans Inf Theory*. 1975;21(1):90-93. <https://doi.org/10.1109/TIT.1975.1055325>
22. Wirsing M, Dammann A, Raulefs R. Designing a Ranging Signal for use with VDE R-Mode. In: *Proceedings IEEE/ION Position, Location and Navigation Symposium (PLANS)*; 2020:822-826.
23. ITU-R Recommendation P.1546-6: Method for point-to-area predictions for terrestrial services in the frequency range 30 MHz to 4000 MHz. 2019.
24. Dammann A, Raulefs R, Zhang S. On Prospects of Positioning in 5G. In: *Proceedings IEEE International Conference on Communication Workshop (ICCW)*. 2015
25. Kay SM. *Fundamentals of Statistical Processing, Volume I: Estimation Theory* ch. 13. Prentice Hall PTR; 1993.
26. Julier SJ, Uhlmann JK. New extension of the Kalman filter to nonlinear systems. In: *Proceedings Signal Processing, Sensor Fusion, and Target Recognition*. Vol.3068; 1997:182-193.
27. Rieck C, Gewies S, Grundhöfer L, Hoppe M. Synchronization of R-Mode Base Stations. In: *Proceedings Joint Conference of the IEEE International Frequency Control Symposium and International Symposium on Applications of Ferroelectrics (IFCS-ISAF)*. 2020; Keystone, CO, USA

AUTHOR BIOGRAPHIES



Markus Wirsing received the Master of Science degree in Electrical Engineering from the University of Ulm, Germany, in 2018. In 2018, he joined the Institute of Communications and Navigation of the German Aerospace Center (DLR) as a research staff member and to pursue a PhD. His research interest and activities include signal design and signal processing for maritime wireless communication and navigation systems.



Armin Dammann received the Dipl.-Ing. (M.Sc.) and Dr.-Ing. (Ph.D.) degrees in Electrical Engineering from the University of Ulm, Germany, in 1997 and 2005, respectively. In 1997, he joined the Institute of Communications and Navigation of the German Aerospace Center (DLR) as a research staff member. Since 2005, he is head of the Mobile Radio Transmission Research Group. His research interest and activities include signal design and signal processing for terrestrial wireless communication and navigation systems. In these fields, he has been active in several EU projects, for example, WINNER, WHERE, and WHERE2. He is lecturer at the Technical University of Munich for “Robot and Swarm Navigation.”



Ronald Raulefs is senior researcher and project manager at the Institute of Communications and Navigation of the German Aerospace Center (DLR) in Wessling, Germany. He received the Dr.-Ing. degree from the University of Erlangen-Nuremberg, Germany, in 2008. He has been a visiting researcher at the City University of Hong Kong in September of 2004. He initiated and coordinated the EU projects WHERE and WHERE2. He holds numerous patents in the area of mobile communications and radio-based localization. His current research interests include various signal processing aspects of mobile and maritime radio communications and localization.

How to cite this article: Wirsing M, Dammann A, Raulefs R. VDES R-Mode performance analysis and experimental results. *Int J Satell Commun Network*. 2021;1-20. doi:10.1002/sat.1424